Desalination and Water Treatment
www.deswater.com

doi: 10.5004/dwt.2018.22109

106 (2018) 98–107
February

Designing of zinc based coordination complex [Zn(bpeb)(OHbdc)].DMF for industrial wastewater treatment

Saira Mansab[a,*], Sana Zulfiqar[a], Fatima Tariq[a], Nosheen Ayub[a], Kousar Parveen[a], Uzaira Rafique[a], Muhammad Javed Akhtar[b]

[a]*Department of Environmental Sciences, Fatima Jinnah Women University, The Mall, Rawalpindi, Pakistan, email: saira.mansab90@gmail.com (S. Mansab), sanazulfiqar1989@gmail.com (S. Zulfiqar), fatimatariq86@gmail.com (F. Tariq), nosheen.ayub@gmail.com (N. Ayub), kosar_ahmed111@yahoo.com (K. Parveen), uzairaiqbal@yahoo.com (U. Rafique)*
[b]*Physics Division, Pakistan Institute of Nuclear Science and Technology, P.O. Nilore, Islamabad, Pakistan, email: javedakhtar6@gmail.com (M.J. Akhtar)*

Received 29 September 2017; Accepted 23 February 2018

ABSTRACT

Clean water demand is one of the main subject that need to be considered after continuous generation of pollution due to rapid industrialization. Thus, efforts have been congregated for the decontamination of wastewater to address the severe clean water shortage. Zinc metal coordination complex was synthesized using the bipyridyl spacer ligand along with hydroxy dicarboxylate as secondary ligand. The 3D coordination complex was characterized using FTIR, ^{1}H NMR, elemental analysis, thermogravimetric analysis and powder XRD. Thermogravimetric analysis and BET analysis depicted high thermal stability and surface area that make it suitable for adsorption experiments. Batch adsorption experiments were conducted for 60 min at varying doses (5 mg, 10 mg and 15 mg) and temperatures (25°C, 50°C, and 70°C) for the removal of azo dyes (Congo Red, Crystal Violet, Methyl Orange). Percentage removal efficiency of azo dyes was in the order of Congo Red (85%) > Crystal Violet (65%) > Methyl Orange (21%). The adsorbent was proved to be effective for removal of pollutants from industrial wastewater with average percent removal of 71% for textile waste. Regeneration and desorption experiment indicated the reuse of synthesized adsorbent for multiple cycles with desorption percentage upto 28%.

Keywords: Coordination complex; Azo dyes; Congo red; Methyl Orange; Crystal Violet

1. Introduction

Industrialization has increased the issue of environmental pollution up to toxic level. These pollutants persist in the environment for long time and thus their removal from the environment is more challenging. Many of them are toxic metals and organic chemicals which persist in environment for long time and thus their removal from environmental components is more challenging [1]. These pollutants include heavy metals, organic dyes and persistent organic pollutants. Biodegradation of these pollutants is very resistive and thus can be easily accumulated in the food chain because of low water solubility and electrochemical stability [2]. Organic dyes pollution is mainly generated from textile pharmaceutical, paper and pulp and bleaching industries from where it is transferred to natural water resources and waste streams. Major pollutants are mostly release from textile industries in the form of dyes, heavy metals, PAHs and contaminate in big ratio for water pollution. Out of its total usage about 25% of them are lost during dyeing process which directly discharges as waste effluent into different environmental components [3]. These dyes not only change the color of water bodies but also breakdown into toxic byproducts of polyaromatic hydrocarbons such as benzidine and naphthalene which are carcinogenic in nature [4].

*Corresponding author.

Metal organic coordination complexes have proved to be efficient adsorbents for removal of environmental pollutants due to high porosity and surface area. These porous coordination polymers consists of a central atom (metal), surrounded with array of atoms or groups of atoms (ligands) [5]. These compounds have been found to possess unique properties. One of the striking feature is their low density, which provides them with high surface areas and porosities. There rigid structure provides them high thermal stability to be used for environmental applications i.e. for sensing of different compounds [6].

Dimensions and topology of the complex can be tuned by modifying the molecular structure of organic ligand or by affixing different substituents on organic ligand and hence new structures can be created [7]. One of the interesting structure is pillared layered that can be formed using bipyridyl spacer ligand, dicarboxylate compound and metal ions. Using the substituted carboxylic group such as amino terephthalic acid provides addition site for attracting the acidic guest molecules to be used for removal of different pollutants [8].

The present study focuses on synthesis of porous coordination polymer Zn(bpeb)(OHbdc)].DMF via solvothermal method. The synthesized complex is further used for removal of organic dyes from wastewater.

2. Materials and methods

All chemicals were purchased from commercial source (Sigma Aldrich) and used as received. All solvents used were of reagent grade. The 1,4-bis[2-(4-pyridyl)ethenyl]benzene (bpeb) ligand was synthesized by the reported procedure [9]. Elemental analyses were carried out on using Elementar vario MICRO cube for CHNS analysis. Thermogravimetric analyses were recorded in a TA Instruments TGA-Q50 thermogravimetric analyzer. Samples were heated at a constant rate of 5°C min^{-1} from room temperature to 700°C and in a continuous flow nitrogen atmosphere. The FT-IR spectra were recorded using FTS165 Bio-Rad FT-IR spectrometer with KBr pellets. NMR analysis was conducted using Bruker A300 instrument. Surface area of the complex is determined through Brunauer, Emmett Teller(BET) adsorption method using Micromeritics Tristar 3000 sorption analyser.

3. Experimental

3.1. Preparation of Zn(bpeb)(OHbdc)].DMF

A mixture of bpeb (20 mg, 0.07 mmol), 2-hydroxy terephthalic acid (OHbdc) (12.74 mg, 0.07 mmol), and $Zn(NO_3)_2$ (13.32 mg, 0.07 mmol) was dissolved in DMF (3 mL), H_2O (1 mL), DMSO (1 mL). It was followed with addition of 3 drops of NaOH and then poured in a 5 mL glass tube. The tube was sealed and kept at 120°C for 48 h, followed by cooling to room temperature over 10 h. Yellow needle shaped crystals obtained were extracted under optical microscope and washed with ethanol and water. Yield: (31 mg) 73%.

3.2. Batch adsorption experiments

The experiments of azo dyes (methyl orange, congo red and crystal violet) adsorption by synthesized coordination complex were performed in batch conditions. The effect of various parameters, reaction time, temperature and pH was investigated. Stock solution of each dye (1000 mg/L) was prepared by dissolution of 1 g of adsorbate in 1 L of distilled water. 10 mg of adsorbent dose was added to 50 ml of each dye working solution (0.5 mg/L). The solution temperature was adjusted using thermocoupled hot plate. The pH of methyl orange was adjusted using 0.1 N NaOH and HCl. All experiments were run on UV-visible spectrophotometer (UV-1601-Schimadzu, Japan). The absorbance of Methyl Orange, Congo Red, and Crystal Violet was recorded at 465 nm, 497 nm, and 590 nm, respectively after full spectral scan. The adsorption (percentage removal) was determined from the constructed calibration curve of each dye using following equation.

$$\%R = \frac{C_i - C_t}{C_i} \times 100 \tag{1}$$

Kinetic models [pseudo first order [Eq. (2)], first order [Eq. (3)], pseudo second order [Eq. (4)] and intraparticle diffusion [Eq. (5)] and adsorption isotherms [Langmuir [Eq. (6)] and Freundlich [Eq. (7)]] were applied on the experimental results to find out rate and mode of adsorption.

$$\frac{C_e}{q_e} = \frac{1}{q_{max} K_L} + \frac{C_e}{q_{max}} \tag{2}$$

$$\log q_e = \log K_F + \frac{1}{n} \log C_e \tag{3}$$

$$\log(q_e - q) = \log q_e - \frac{k_1 t}{2.303} \tag{4}$$

$$\log C_t = \frac{k_1}{2.303} t + \log C_o \tag{5}$$

$$\frac{1}{q_t} = \frac{1}{k_2 q_e^2} + \frac{1}{q_e} t \tag{6}$$

$$\log R = \log k_{id} + a \log(t) \tag{7}$$

3.3. Regeneration experiment

Regeneration studies of adsorbent were conducted by making the contact between 300 mg of coordination complex and 15 mg/L concentration of Congo red dye. After completion of adsorption, anhydrous ethanol was added to the saturated adsorbent, shaken vigorously and soaked in solvent for one day to extract the adsorbed dye. Regeneration process was done using 1 M HCl solution followed by addition of ethanol/H_2O (1:1). The mixture was stirred and then equivalent amount of NaOH solution was slowly added and stirred for 1 h. The precipitated were filtered and washed several times with ethanol and oven dried at 120°C and analysed with PXRD for regeneration study (yield: 257 mg, 87%).

4. Results and discussion

4.1. Characterization

4.1.1. NMR analysis

^{1}H NMR spectrum, δ, ppm: 7.20 (d, *J* = 8.2 Hz, 1H), 7.51 (s, 1H), 7.59 (d, *J* = 16.3 Hz, 1H), 7.81 (s, 1H), 7.83 (s, 1H), 7.91 (s, 1H), 8.04 (d, *J* = 15.7 Hz, 1H), 8.19 (d, *J* = 6.7 Hz, 1H), 8.82 (d, *J* = 6.6 Hz, 1H). ^{1}H-NMR spectra showed the presence of both spacer ligand and carboxylate group which indicated the successful synthesis of framework structure. It was found from the integration values that the ligands binded to the zinc metal in 1:1:1 for bpeb, OHbdc and DMF, respectively (Fig. 1).

4.1.2. Elemental analysis

The formula predicted from the results of elemental analysis is found to be ZnC31H28N3O6 i.e. [Zn(bpeb)(OHbdc)].DMF which should have diamondiod structural arrangements in which two nitrogen of bpeb ligand and two oxygen of OHbdc ligand will bind with one zinc metal (Table 1).

4.1.3. TGA analysis

TGA results revealed that for complex a constant weight loss of 11.78 wt% till 200°C, which is ascribed to the removal of DMF molecules (calculated 12.1%) after that the framework collapsed near 250°C. The complete decomposition of complex occurred at 500°C. Weight loss of DMF calculated from the formula predicted by CHNS analysis was quite similar to the percent weight loss obtained from TGA graph which verify the predicted formula (Fig. 2).

4.1.4. FTIR analysis

It is revealed from the IR spectra of coordination complex that the appearance of broad peak at 3482 cm^{-1} is attributed to the OH stretching peak of the OHbdc ligand. The peak present at 3100 cm^{-1} is ascribed to aromatic CH stretching while small peak at 2937 cm^{-1} is linked to CH stretching of the alkyl groups present between the aromatic pyridyl and benzene rings. The peak at 1678 cm^{-1} is associated with the carboxylic group of the OHbdc ligand. Sharp C=N stretching peak of pyridyl group is appeared at 1591 cm^{-1} in bpeb ligand, while it is missing in coordination complex due to bonding of metal with N of pyridyl group. C=C peak can be observed at 1508 cm^{-1}. Sharp CN stretching peaks at 1278 cm^{-1} justifies the presence of bpeb ligand. The peaks associated with in and out of plane OH are observed at 1400 cm^{-1} and 973 cm^{-1}, respectively. CH in

Table 1
CHNS analysis of complex verses calculated percentages

	C%	H%	N%
CHN analysis	61.51	4.23	6.54
Calculated	61.65	4.67	6.96

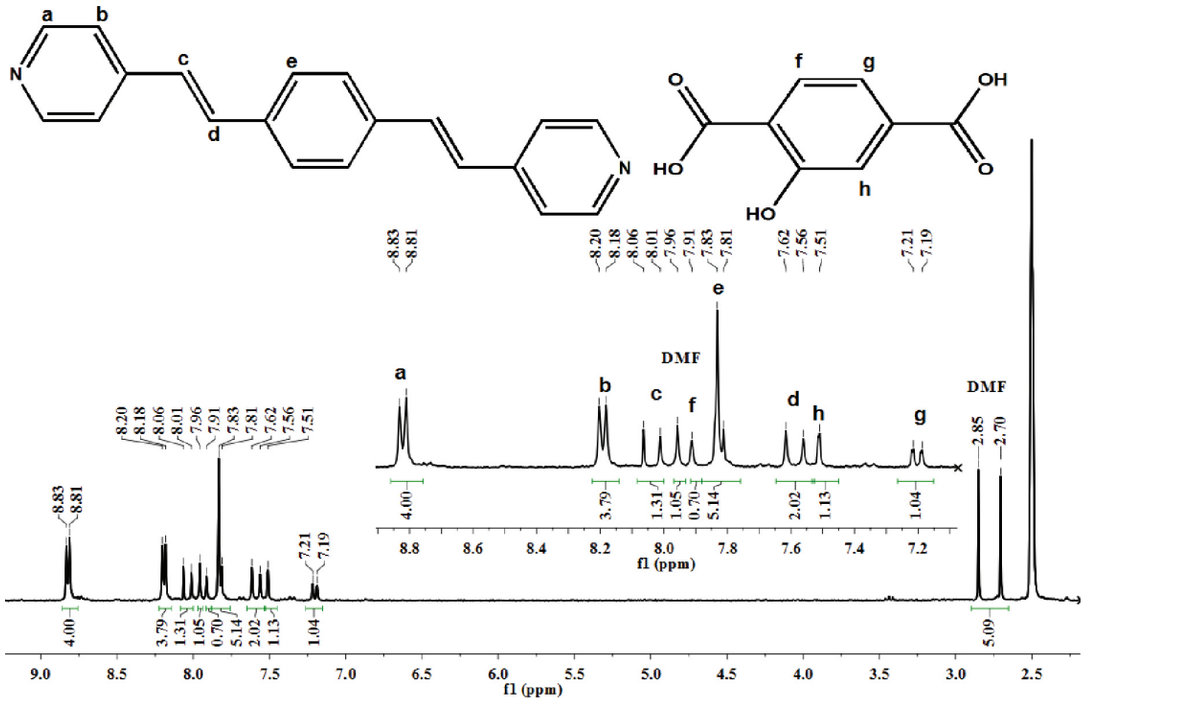

Fig. 1. ^{1}H NMR spectra of complex in DMSO-*d*6 with a small drop of trifloroacetic acid to dissolve the crystals.

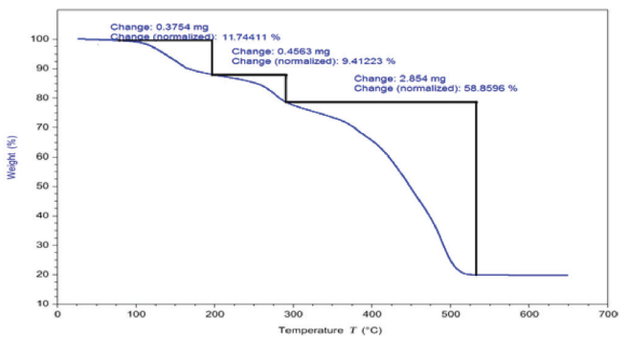

Fig. 2. TGA curve of complex under air flow with heating rate of 5°C·min^{-1}.

and out of plane bending vibrations are detected at 1440 and 828 cm^{-1} (Fig. 3).

4.1.5. XRD analysis

Powder XRD pattern presented the crystalline nature of product and the comparison of powder XRD data with the reported simulated pattern was quiet similar which verifies the successful synthesis of the coordination complex [10] (Fig. 4).

4.1.6. Structural description

The structure predicted from the above analysis shows a diamond like arrangement of the framework in which tetrahedral zinc is coordinated with the two nitrogen atoms of the bpeb ligand and two oxygen atoms of the OHbdc ligand to form a zigzag chain (Figs. 5 and 6). These chains are packed in the form of sheets one above the other due to OHbdc chain in which bpeb ligand is slip-staked on each other. Such type of packing forms a 3D network structure (Fig. 7).

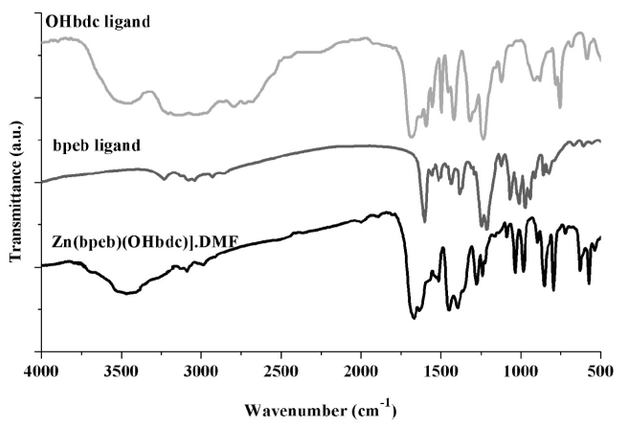

Fig. 3. FTIR spectral overlay of complex and bpeb ligand.

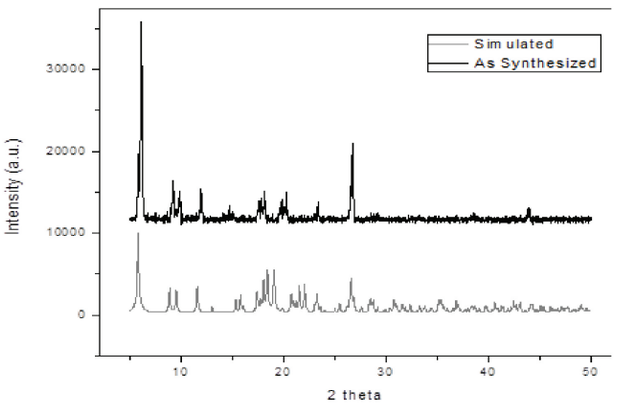

Fig. 4. PXRD patterns of complex and simulated from the single crystal data of literature.

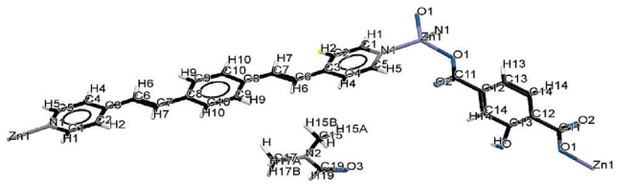

Fig. 5. Perspective view of Zn binding with ligands.

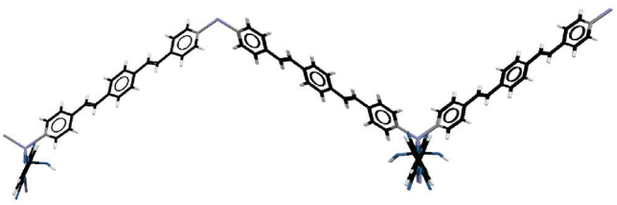

Fig. 6. Zigzag alignment of bpeb ligand in coordination complex.

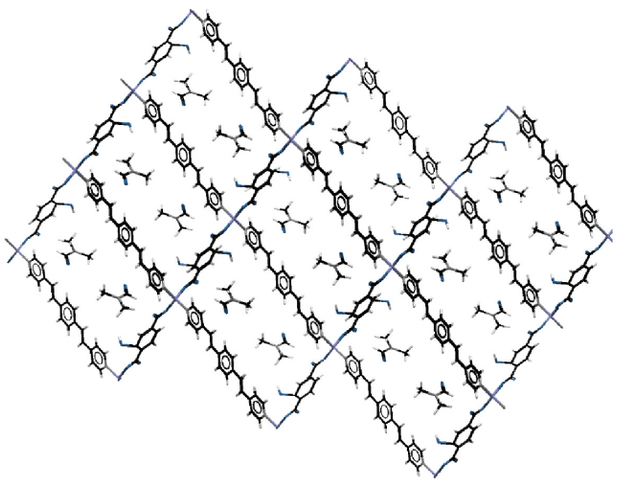

Fig. 7. Network arrangement of ligands in coordination complex.

4.1.7. BET surface area analysis

Nitrogen sorption-desorption method was used for determining pore volume. The sample was preheated for 2 h at 180°C under nitrogen gas flow to remove moisture prior to BET analysis. The compound possesses 0.514 cm^3/g pore volume with BET surface area 1587 m^2/g (Table 2).

It is depicted from the graph that the synthesized coordination follows type II sorption isotherm related to monolayer and multilayer sorption. The complex showed maximum saturation capacity at 314 cm^3/g. Desorption followed exactly the adsorption pattern which indicates its efficient of reusability (Fig. 8).

Presence of voids and additional functional group (OH) can make this coordination complex a good adsorbent for removal of organic pollutants.

Table 2
Surface area of [Zn(bpeb)(OHbdc)].DMF coordination complex

$S_{BET,}$ m^2/g	1587
$S_{Langmuir}$, m^2/g	1767
V_{tot}, cm^3/g	0.687
$V_{micropores}$, cm^3/g	0.514

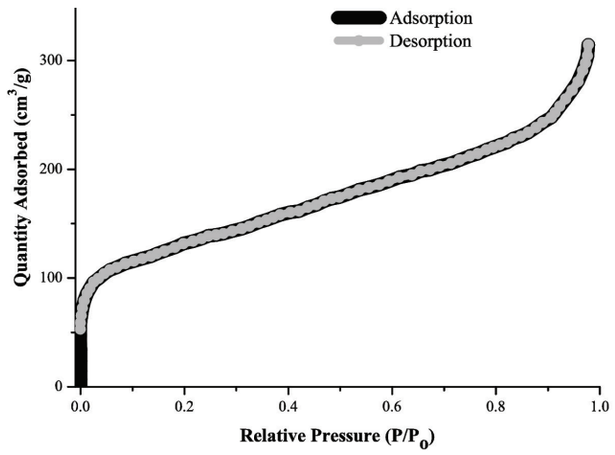

Fig. 8. Nitrogen adsorption isotherm of [Zn(bpeb)(OHbdc)]. DMF coordination complex.

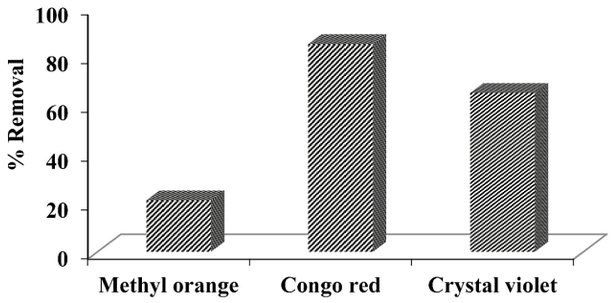

Fig. 9. Removal (%) of azo dyes using synthesized adsorbent.

4.2. Application for removal of dyes

Three organic azo dyes (Congo Red, Crystal Violet, Methyl Orange) were selected for batch adsorption studies. The purpose behind selection of these three azo dyes was their rich toxicity profile as carcinogens due to different pH nature they possess. Congo as an anionic dye, crystal violet as cationic nature while Methyl orange as pH indicator is mostly used by textile industries and release as major pollutants in downstreams. For wastewater treatment, the above mentioned azo dyes were remediated using synthesized adsorbent (coordination complex).The results indicate good adsorptive removal for Congo Red and Crystal Violet as compared to Methyl Orange with removal trend observed in the order of Congo Red > Crystal violet > Methyl Orange. The reason for high percentage removal of anionic dye can be attributed towards the Cation-Anion interaction of coordination complex with Congo red [11] in duration of 1 h. As the Zinc metal possess positive charge on its surface which creates electrostatic interaction towards the anionic Congo Red. Besides, Crystal Violet was also removed efficiently which is supported by the presence of COO^- and OH groups on adsorbent surface that may favor crystal violet adsorption on the surface due to electrostatic interaction [12]. On the other hand, potential of adsorbent for methyl orange removal was very less may be due to pH depending nature of adsorbate [13]. As in aqueous solution methyl orange exists in its basic form and thus due to anionic-anionic repulsion its adsorption was less [14].

4.2.1. Effect of contact time

The adsorbate-adsorbent interactions were studied with respect to contact time. Experiments were conducted in close batch mode of 60 min, at optimum dose (10 mg) and concentration (0.5 mg/L) (Fig. 10). It can be seen that first dynamic equilibrium was observed near 15 min in case of methyl orange, Congo red and crystal violet, followed by desorption phenomenon till 25 min unless second equilibrium was attained. Rapid increase in the removal efficiency at initial time is attributed to presence of abundant binding sites for adsorption [15].

The increase in % removal for Congo Red in first 13 min is due to the availability of maximum sites in initial time. After 13 min there was no further increase in removal of dye and equilibrium was observed, subsequently at

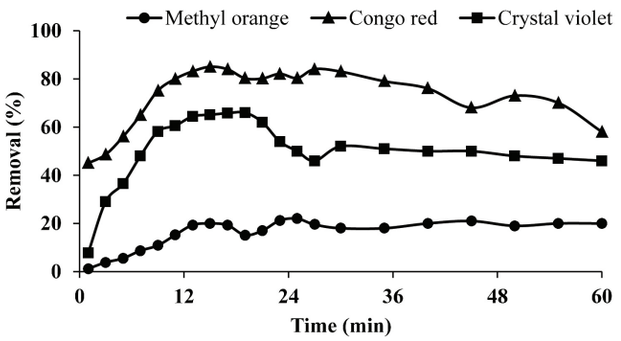

Fig. 10. Effect of contact time for removal of dyes.

17 min desorption process occur with no further noticeable enhancement of adsorption due to occupied binding sites.

Adsorption removal of crystal violet with relation to contact time also presented the increasing trend upto 13 min and equilibrium is maintained till 20 min. After that desorption process started till 27 min with no further increase in removal.

4.2.2. Effect of temperature

Batch experiments were conducted at three different temperatures, i.e., 25°C, 50°C and 70°C for 5 mg dose and 0.03 mg/L initial concentration. The results revealed that as increases from 25°C to 50°C, adsorption of azo dyes increases followed by decrease in removal till 70°C as shown in Fig. 11. The increase in percent removal could be result of decrease in particle density of adsorbent (coordination complex), creating more reactive sites at surface and thus increase the penetration of guest molecules in micropores [16]. In the literature, the increase in temperature cause pore size enlargement thus adsorption capacity increase. Similarly, the decrease in adsorption till 70°C can be due to increase in kinetic energy which makes the reaction exothermic and thus dye desorbs at elevated temperature [17].

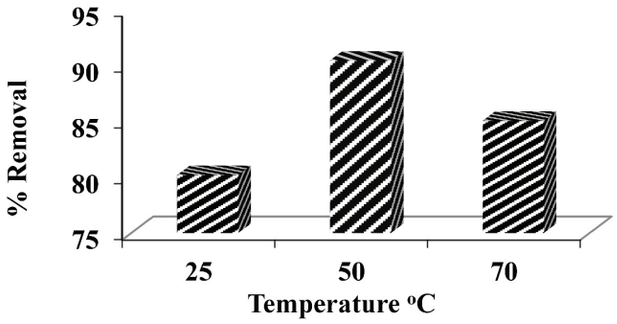

Fig. 11. Effect of temperature for removal of Congo Red.

4.2.3. Effect of solution pH

Methyl orange was investigated to study pH variations effect on adsorption performance (Fig. 12). As methyl orange is a pH indicator dye so its adsorption varies with the slight variation in the pH. It is found that when the pH of the aqueous solution was change to acidic, the adsorption of the methyl orange was increased more prominently, while at basic pH (10 and 12) the maximum removal percentage was only 22% and 17%, respectively. It has been reported that at acidic pH, the surface of the adsorbent is activated by the acid in the solution and the anionic dye become protonated thus adsorption efficiency increases [18]. Furthermore. at higher pH, the conjugation system of the dye breaks down with loss of proton due to pi bond delocalization, and molecule rearrange itself to form anionic species. These negatively charged ion neutralized the positive charges and repulsion of the dye occur by the negative charge of the adsorbent surface [19].

4.2.4. Removal of dyes from textile effluents

Textile effluent from local industry was collected and full scanned on UV-Visible spectrophotometer. Full scan confirmed the presence of Congo Red dye with maximum absorbance at 495 nm wavelength. Total concentration found from calibration curve was observed to be 0.02 mg/L. Effect of dose was studied and maximum removal was observed to be 71% in 1 h contact time, which was less as compared to experimental batch (Fig. 13). This may be the result of hindrance caused by other particles present in wastewater.

4.2.5. Adsorption kinetics

Kinetic models give an insight for better understanding of adsorption transport mechanism. Kinetic data is used to predict the rate at which the adsorbate is removed from the solution. The adsorption kinetics was applied on experimental results to find the best fit model (Table 3). Results supported pseudo-second order reaction due to linear fitting of models and close integrity of correlation coefficient (R^2) can be attributed to sorption equilibrium capacity of the solid phase (Figs. 14 and 15) [1,20]. Predicted kinetic model also proposed that the rate of binding site occupancy is proportional to the square of number of the unoccupied sites [21].

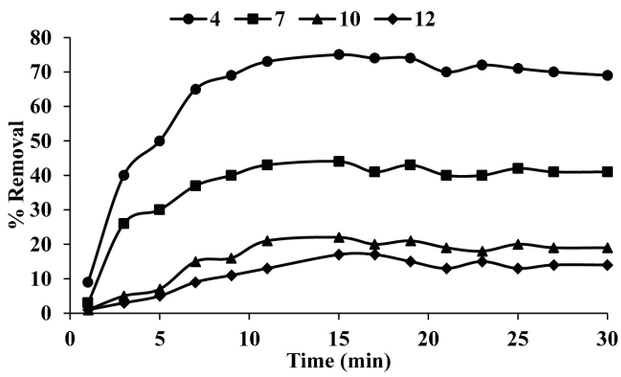

Fig. 12. Effect of pH for removal of methyl orange.

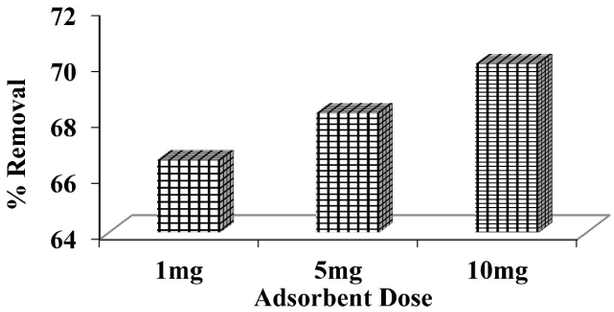

Fig. 13. Removal of Congo Red from textile wastewater.

Table 3
Kinetics studies of adsorption for azo dyes removal using [Zn(bpeb)(OHbdc)].DMF

Adsorbates	1st order			Pseudo-1st			Pseudo-2nd			Intra-particle		
	C_o	K_1	R^2	K_1	$q_{e\,cal}$	R^2	K_2	$q_{e\,cal}$	R^2	A	K_{id}	R^2
Methyl Orange	– 0.435	0.0007	0.297	–0.004	–2.167	0.412	37.979	25.829	0.992	–0.004	1.268	0.322
Congo Red	–1.951	0.002	0.035	36.15	–30.73	0.000	25.011	30.944	0.990	7E–05	1.731	0.000
Crystal Violet	–1.736	0.004	0.527	–0.000	0.037	0.684	29.441	28.07	0.996	–0.003	1.644	0.619

4.2.6. Adsorption isotherms

Langmuir model was used to study the physiosorption while Freundlich model was used to investigate the adsorption on heterogeneous surfaces of multilayer surface [22]. Langmuir and Freundlich isothermic model describes the mode of adsorption of dyes onto synthesized coordination complex (Table 4). Linearity of the isotherm for both models depicted that adsorption was occurred both on the surface and bulk (Figs. 15 and 16).

4.2.7. Regeneration studies

PXRD studies were conducted to analyse the structural changes and regeneration ability after adsorption of guest molecules. It can be seen from Fig. 17 that the XRD peaks for the degraded coordination complex has different 2-theta value that is attributed to the geometrical changes resulting from the chemical sorption of the dye molecules. It has been reported that this chemical sorption can be either through the electrostatic interactions on the positively charged metal sites or it may be appeared due to presence of functional group on the ligand [23]. PXRD pattern obtained after regeneration experiment clearly indicated the successful desorption of the Congo Red from complex and the geometry of the framework is regained.

After successful regeneration, the complex was further tested for its reusability. For this purpose, adsorption experiments were conducted on Congo Red dye for five repeated cycles (Fig. 18). It has been found that, despite the slight drop in the adsorption efficiency after first cycle, the complex showed considerable adsorption upto 5 cycles. These results reveals that the synthesized coordination complex can be efficiency reused and regenerated for multiple times.

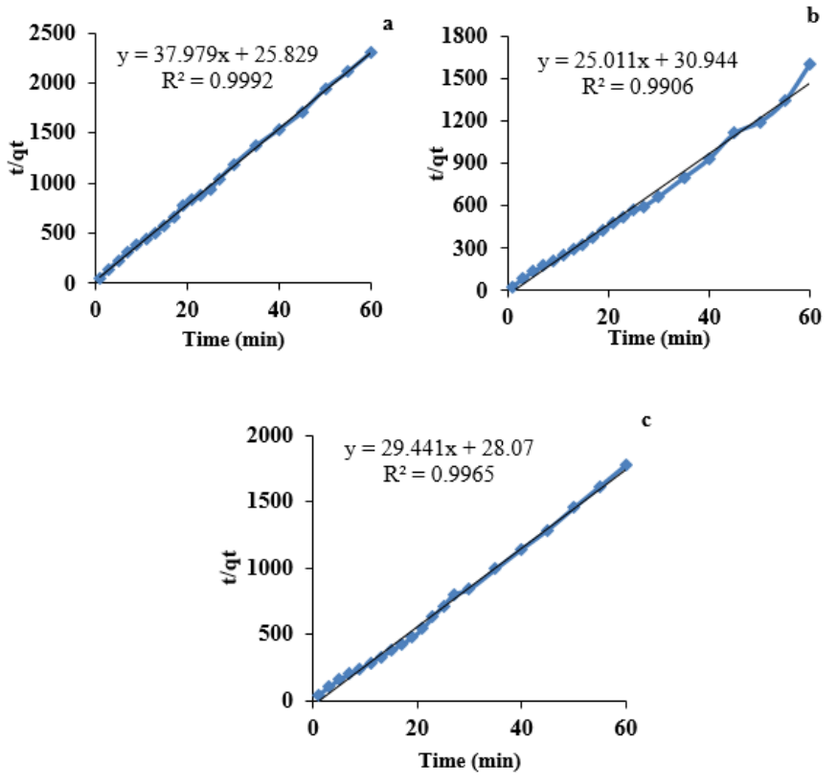

Fig. 14. Pseudo second order kinetics for the adsorption of (a) Methyl Orange (b) Congo Red (c) Crystal Violet.

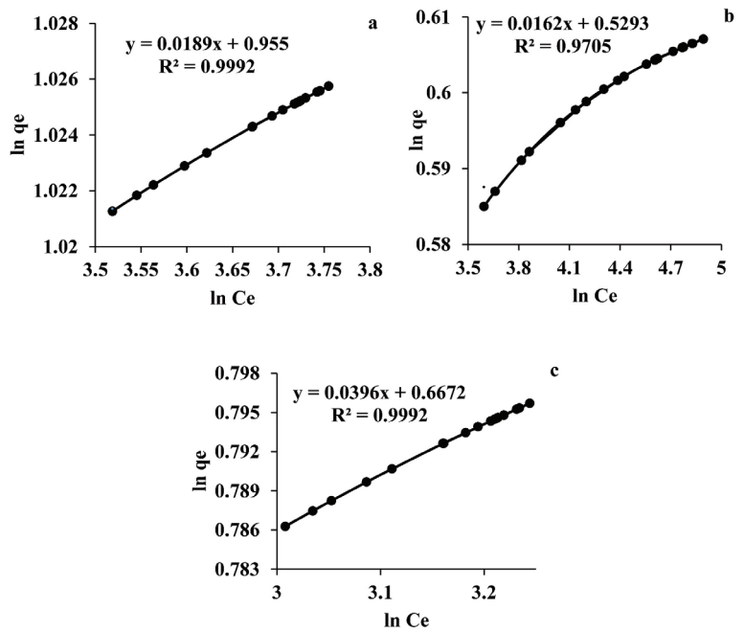

Fig. 15. Freundlich isotherms for the adsorption of (a) Methyl Orange (b) Congo Red (c) Crystal Violet.

Table 4
Adsorption isotherms for azo dyes removal using [Zn(bpeb)(OHbdc)].DMF coordination complex

Adsorbates	Freundlich			Langmuir		
	K_F	n	R^2	q_m	K_L	R^2
Methyl Orange	1.019	1.047	0.999	1830.8	2.731	0.998
Congo Red	1.016	1.889	0.9705	5608.5	1.783	0.999
Crystal Violet	1.040	1.498	0.999	589.125	2.1217	0.998

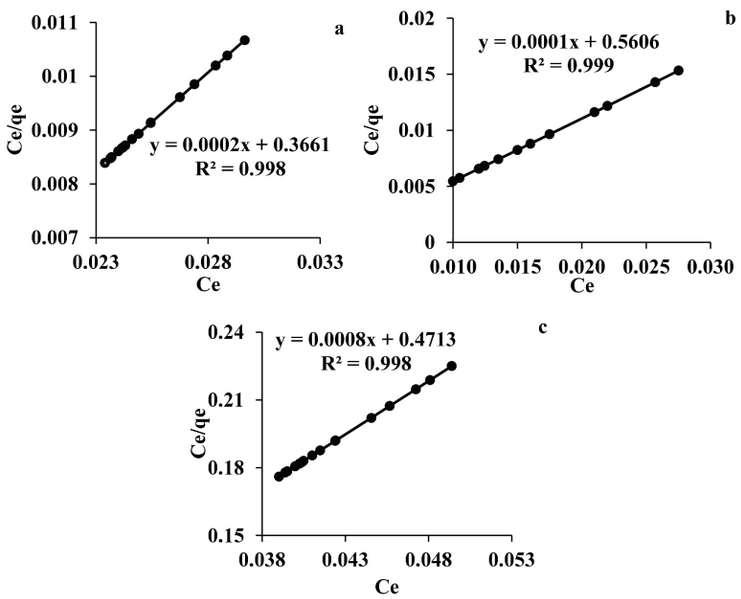

Fig. 16. Langmiur isotherms for the adsorption of (a) Methyl Orange (b) Congo Red (c) Crystal Violet.

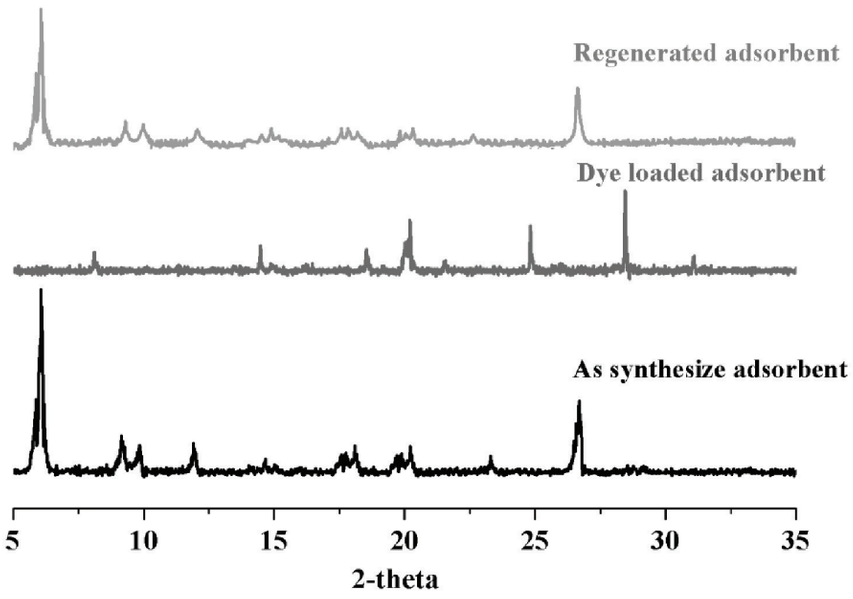

Fig. 17. PXRD of as-synthesized, degraded and regenerated coordination complex.

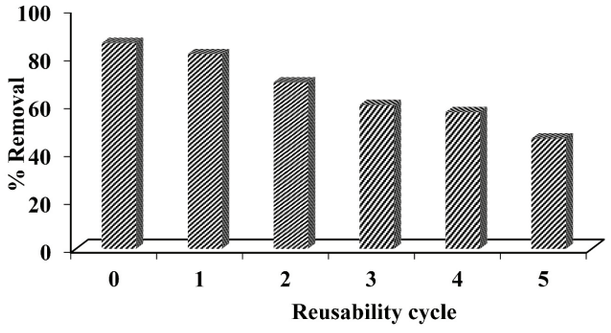

Fig. 18. Reusability cycles of coordination complex.

Table 5
Percentages of adsorbed and desorbed dye

Concentration of dye (mg/L)	Adsorption (%)	Desorption (%)
0.05	23.6	BDL
0.07	45.8	3.3
0.1	56.1	9.6
0.5	81.3	21.2
0.7	87.9	26.1
1.0	92.4	28.2

Desorption of adsorbed dye was investigated at different initial concentrations of the adsorbate by analysing the filtrate of desorbed dye (Table 5) [20]. It was found that with increasing amount of adsorption, the percent recovery of the sorbed dye was increased. Moreover, the overall percentage of desorption was low due to chemical binding of the dye with the coordination complex that made desorption difficult.

5. Conclusion

A microporous Zn(bpeb)(OHbdc)].DMF 3D coordination complex was synthesized under solvothermal conditions. Different characterization techniques were used to predict its structure and void volume. BET results represented the high surface area and pore volume. So, the complex was further used as adsorbent for removal of azo dyes through batch adsorption experiments. Adsorption experiments showed good removal efficiency for Congo red and crystal violet but less efficiency for methyl orange. The sorption equilibrium was reached in about 15 min for all dyes. Fitness of isothermal models supported the multiplayer adsorption phenomena. The synthesized coordination complex was also proved efficient adsorbent for removal of dye from wastewater with adsorption percentage upto 71%. Desorption and Regeneration ability of the synthesized adsorbent predicted its reusability for more than five cycles.

References

[1] K. Parveen, U. Rafique, S.Z. Safi, M.A. Ashraf, A novel method for synthesis of functionalized hybrids and their application for wastewater treatment, Desal. Water Treat., 57 (2016) 161–170.
[2] I. Niţã, M. Iorgulescu, M.F. Spiroiu, M. Ghiurea, C. Petcu, O. Cintezã, The adsorption of heavy metal ions on porous cal-

cium alginate microparticles, An. Univ. Bucuresti. Chimie., 1 (2007) 59–67.
[3] E. Haque, J.E. Lee, I.T. Jang, Y.K. Hwang, J.S. Chang, J. Jegal, S.H. Jhung, Adsorptive removal of methyl orange from aqueous solution with metal-organic frameworks, porous chromium-benzenedicarboxylate, J. Hazard. Mater., 181 (2010) 535–542.
[4] M. Saira, R. Uzaira, H. Noman ul, Synthesis of Ni based metal organic frameworks and its applications for removal of polyaromatic hydrocarbons, Int. J. Innov. App. Stud., 15 (2015) 443–451.
[5] S.R. Batten, N.R. Champness, X.M. Chen, J. Garcia-Martinez, S. Kitagawa, L. Öhrström, M. O'Keeffe, M.P. Suh, J. Reedijk, Coordination polymers, metal–organic frameworks and the need for terminology guidelines, Cryst. Eng. Comm., 14 (2012) 3001–3004.
[6] H. Li, M. Eddaoudi, M. O'Keeffe, O.M. Yaghi, Design and synthesis of an exceptionally stable and highly porous metal-organic framework, Nature 402 (1999) 276.
[7] H. Wang, S.J. Liu, D. Tian, J.M. Jia, T.L. Hu, Temperature-dependent structures of lanthanide metal–organic frameworks based on furan-2, 5-dicarboxylate and oxalate, Cryst. Growth Des., 12 (2012) 3263–3270.
[8] S. Kitagawa, R. Matsuda, Chemistry of coordination space of porous coordination polymers, Coord. Chem. Rev. 251 (2007) 2490–2509.
[9] A. Gutov, E. Rusanov, L. Chepeleva, S. Garasevich, A. Ryabitskii, A. Chernega, New viologen analogs: 1, 4-bis [2-(pyridin-4-yl) ethenyl] benzene quaternary salts, Russ. J. Gen. Chem., 79 (2009) 1513–1518.
[10] I.H. Park, C.E. Mulijanto, H.H. Lee, Y. Kang, E. Lee, A. Chanthapally, S.S. Lee, J.J. Vittal, Influence of interpenetration in diamondoid metal–organic frameworks on the photoreactivity and sensing properties, Cryst. Growth Des. 16 (2016) 2504–2508.
[11] K.G. Bhattacharyya, A. Sharma, Kinetics and thermodynamics of methylene blue adsorption on neem (Azadirachta indica) leaf powder, Dyes Pigm., 65 (2005) 51–59.
[12] V.P. Mahida, M.P. Patel, Removal of some most hazardous cationic dyes using novel poly (NIPAAm/AA/N-allylisatin) nanohydrogel, Arab. J. Chem., 9 (2016) 430–442.
[13] M.J. Iqbal, M.N. Ashiq, Thermodynamics and kinetics of adsorption of dyes from aqueous media onto alumina, J. Chem. Soc. Pak., 32 (2010) 419–428.
[14] A.A. Jalil, S. Triwahyono, S.H. Adam, N.D. Rahim, M.A.A. Aziz, N.H.H. Hairom, N.A.M. Razali, M.A. Abidin, M.K.A. Mohamadiah, Adsorption of methyl orange from aqueous solution onto calcined Lapindo volcanic mud, J. Hazard. Mater., 181 (2010) 755–762.
[15] B. Hameed, A. Ahmad, Batch adsorption of methylene blue from aqueous solution by garlic peel, an agricultural waste biomass, J. Hazard. Mater., 164 (2009) 870–875.
[16] M. Al-Ghouti, M. Khraisheh, M. Ahmad, S. Allen, Thermodynamic behaviour and the effect of temperature on the removal of dyes from aqueous solution using modified diatomite: a kinetic study, J. Colloid Interface Sci., 287 (2005) 6–13.
[17] Y.S. Al-Degs, M.I. El-Barghouthi, A.H. El-Sheikh, G.M. Walker, Effect of solution pH, ionic strength, and temperature on adsorption behavior of reactive dyes on activated carbon, Dyes Pigm., 77 (2008) 16–23.
[18] A. Zhang, Y. Fang, Influence of adsorption orientation of methyl orange on silver colloids by Raman and fluorescence spectroscopy: pH effect, Chem. Phys., 331 (2006) 55–60.
[19] F.P. Sejie, M.S. Nadiye-Tabbiruka, Removal of methyl orange (MO) from water by adsorption onto modified local clay (kaolinite), Phys. Chem., 6 (2016) 39–48.
[20] V. Vimonses, S. Lei, B. Jin, C.W. Chow, C. Saint, Kinetic study and equilibrium isotherm analysis of Congo Red adsorption by clay materials, Chem. Eng. J., 148 (2009) 354–364.
[21] S. Schiewer, S.B. Patil, Pectin-rich fruit wastes as biosorbents for heavy metal removal: equilibrium and kinetics, Bioresour. Technol., 99 (2008) 1896–1903.
[22] H. Saleem, U. Rafique, R.P. Davies, Investigations on post-synthetically modified UiO-66-NH2 for the adsorptive removal of heavy metal ions from aqueous solution, Micropor. Mesopor. Mater., 221 (2016) 238–244.
[23] X. Zhu, B. Li, J. Yang, Y. Li, W. Zhao, J. Shi, J. Gu, Effective adsorption and enhanced removal of organophosphorus pesticides from aqueous solution by Zr-based MOFs of UiO-67, ACS Appl. Mater. Interfaces, 7 (2014) 223–231.